*Korean J. Chem. Eng.*, **30**(10), 1867-1875 (2013)
DOI: 10.1007/s11814-013-0138-0

# Development of a model for dimethyl ether non-adiabatic reactors to improve methanol conversion

**Fatemeh Nasrollahi*, Gholamreza Bakeri**†, Ahmad Fauzi Ismail***, Mostafa Rahimnejad**, and Mahdi Imanian******

*Department of Chemical Engineering, University of Tehran, Tehran, Iran
**Faculty of Chemical Engineering, Babol Noshirvani University of Technology, Babol, Iran
***Advanced Membrane Technology Research Centre (AMTEC), Universiti Teknologi Malaysia, 81310 Skudai, Johor, Malaysia
****Department of Mechanical Engineering, Mohajer Technical University, Isfahan, Iran
(*Received 17 February 2013 • accepted 30 July 2013*)

**Abstract**−The modeling of adiabatic and non-adiabatic reactors, using three cooling mediums in the shell side of a shell and tube reactor in cocurrent and countercurrent flow regimes has been conducted. The cooling mediums used in this research are saturated water and methanol feed gas to a reactor which is preheated in the shell side and a special type of oil. The results of adiabatic reactor modeling show good compatibility with the data received from a commercial plant. The results of non-adiabatic reactor modeling showed that more methanol conversion can be achieved in a lower length of reactor, even though in some cases the maximum temperature in the tube side of the reactor is more than the deactivation temperature of the catalyst.

Key words: Dimethyl Ether, DME, Modeling, Non-adiabatic Reactor, Shell and Tube Reactor

## INTRODUCTION

Di-Methyl ether (DME), which is known as a clean fuel, is a colorless and nontoxic compound with one oxygen atom in its structure, which contributes to excellent combustion characteristics of DME and production of less toxic materials such as particulate materials, sulfur dioxide and $NO_x$ during the combustion process. Moreover, higher cetane number of DME compared to conventional diesel fuels and its liquefaction and handling properties have led to the heightened attention to DME as a leading alternative for petroleum-based fuels such as transportation and power plant fuels, stationary fuel cells and liquefied petroleum gas (LPG) [1-3]. Thus, by low-cost mass production of DME, the environmental problems from the expanded energy consumption can be solved.

There are two methods normally employed for DME production namely indirect and direct. The direct method, which has been licensed by companies such as Haldor-Topsoe, JFE and Air Products, has not been commercialized yet [4-6]. The commercial process for DME production is the dehydration of methanol in two steps (indirect method) which two moles of methanol, over an acidic catalyst such as $\gamma$-Alumina and during an exothermic reaction, convert to one mole DME and one mole water. Generally, an adiabatic fixed bed reactor or fluidized bed reactor is used in the indirect method [7], and many researches have been done to investigate the effect of various parameters and catalysts on the performance of these types of reactors [8-10].

Since the deactivation temperature of catalyst places limits on the temperature of the reactor, it must be considered as an important parameter in the design and modeling of a DME reactor. So that, increasing the reaction temperature over the deactivation temperature of the catalyst leads to the sintering of catalyst and formation of hot spot, which damages the catalyst. In addition, decreasing of the temperature below a specific temperature causes adsorption of water vapor on the catalyst surface and hydration of acidic sites of the catalyst which prevents the reaction of methanol over acidic sites of catalyst and reduces the activity of catalyst [9]. The recommended temperature range for methanol dehydration reaction over $\gamma$-Alumina is 260-380 °C.

Several researches have been published for simulation of DME process and modeling of non-adiabatic and adiabatic packed bed reactors. Ng et al. used two different kinetic models for methanol dehydration process and evaluated these models with the obtained experimental data [3]. Lu et al. developed a model for simulation of fluidized-bed reactor for DME synthesis and compared the results with a fixed bed reactor and showed the great advantage of the fluidized-bed reactor compared to fixed-bed or slurry reactors [7]. Lee et al. developed a model for one-step DME synthesis from synthesis gas in a tubular fixed bed reactor and investigated the effects of different arrangement of the catalyst on the results [4]. A model was developed by Liu et al. to simulate a three-phase bubble column reactor for direct synthesis of dimethyl ether from synthesis gas, considering the effect of catalyst sedimentation on the reaction [11]. The DME production via direct method from synthesis gas over a bifunctional catalyst was simulated by modeling of a pipe-shell reactor elsewhere [12]. Among the many researches for evaluation of kinetic parameters and reaction mechanism of DME production [13-17], a new methanol dehydration mechanism using two types of alkali mZSM-5 catalysts was presented by Ha et al. [18]. They also simulated the reactor using a one-dimensional pseudo-homogeneous plug flow model and showed that their proposed reaction rate had good ability in prediction of methanol conversion.

As methanol dehydration is an exothermic reaction, the equilibrium reaction constant and the equilibrium conversion decrease with

†To whom correspondence should be addressed.
E-mail: bakeri@nit.ac.ir, ghr_bakeri@yahoo.com

increasing temperature in the adiabatic reactor. Therefore, controlling the temperature in the non-adiabatic reactor can increase the chemical potential of reaction and provide more conversion of methanol.

In view of further enhancing the performance of DME production, the present work investigates the methanol conversion and DME production in a non-adiabatic reactor in comparison with the adiabatic reactor. The indirect DME production via methanol dehydration over $\gamma$-Alumina is considered. In a non-adiabatic reactor, three different cooling mediums in the shell side of a tubular reactor, which are the saturated water, methanol feed gas and cooling oil in co-current and countercurrent flow regimes, were used to cool the reactor. Furthermore, the temperature limitations for catalyst were considered.

## MODELING

DME reactor modeling is based on the mass, energy and momentum balances. We considered the main methanol dehydration reaction and omitted the side reactions as their conversion is very limited. Considering the high velocity and turbulence of the gas stream along the tubes, the mass transfer resistance between the gas phase and the catalyst surface and the radial distribution of temperature is negligible in comparison with the axial direction and, as a result, a one-dimensional model is used for prediction of concentration and temperature profiles along the reactors [18]. The final equations for mass, energy and momentum balances in adiabatic reactor and in tubes of non-adiabatic reactor are as Eqs. (1)-(3).

$$\frac{dx}{dz}=\frac{-r_{MeOH}\rho_B A_i}{F_{m0}} \tag{1}$$

$$\frac{dT}{dz}=\frac{-A_i\rho_B r_{MeOH}(-\Delta H_{rxn})-q\pi D_i}{\sum_i F_i Cp_i},\quad q=U_i(T-T_{shell}) \tag{2}$$

$$\frac{dP}{dz}=\frac{-f_k G^2(1-\xi)}{D_p\rho_f\xi^3},\quad f_k=1.75+150\frac{1-\xi}{D_pG/\mu} \tag{3}$$

where in the mass balance equation (Eq. (1)), x, $r_{MeOH}$ and $\rho_B$ are methanol conversion, rate of methanol consumption and bulk density of catalyst bed, respectively. $A_i$ is the internal cross sectional area of adiabatic reactor and tubes of non-adiabatic reactor, and $F_{m0}$ is the feed methanol molar flow rate. In this equation, the diffusion term in comparison with the convection term and mass transfer in radial direction in comparison to the axial mass transfer were omitted.

In the energy balance equation (Eq. (2)), $\Delta H_{rxn}$ is the heat of reaction at reaction temperature, q is the transferred heat per unit heat transfer area of tubes, which is zero for adiabatic reactors, and $D_i$ is the internal diameter of tubes. In the momentum balance equation (Eq. (3)), G, $\xi$, $\rho_f$, $\mu$ and $D_p$ are mass flow rate per unit area of reactor inlet, void fraction of catalyst bed, density of fluid flows inside the tubes, fluid viscosity and equivalent diameter of catalyst particles, respectively.

To calculate q, the overall heat transfer coefficient should be obtained through Eqs. (4)-(5) which are written based on the heat transfer resistances in series [19].

$$\frac{1}{U_i}=\frac{1}{h_i}+\frac{A_i}{h_oA_o}+\frac{A_i\ln\frac{D_o}{D_i}}{2\pi KL} \tag{4}$$

$$\frac{1}{h_i}=\frac{1}{h_b}+\frac{1}{h_w} \tag{5}$$

where $h_i$ and $h_o$ are the heat transfer coefficients in the tube side and shell side, respectively and K is the thermal conductivity of tube. To calculate the heat transfer coefficients, experimental correlations, which were more consistent with the geometric and operational conditions of the non-adiabatic reactors were applied, e.g. Eqs. (6)-(7) are used for calculation of the bed and wall sides heat transfer coefficients ($h_b$, $h_w$) for a bed of cylindrical catalysts [19].

$$h_b=\frac{4k_{er}}{R},\quad k_{er}=5+0.1Re_pPr \tag{6}$$

$$h_w=\frac{Nu_wk}{D_p},\quad Nu_w=0.16Re_p^{0.93}(Pr/0.7)^{0.33} \tag{7}$$

Calculation of $h_o$ depends on the cooling media used in the shell side of the tubular non-adiabatic reactor. For saturated water in the shell side, Eq. (8) presented by Gilmour et al. for vertical thermosiphon reboilers [20] was used for the vertical reactors in this study.

$$h_o=\frac{\phi Gp_lG_{gb}}{\left(\frac{D_oG_{gb}}{\mu_l}\right)^{0.3}}\left(\frac{Cp_l\mu_l}{k_l}\right)^{-0.6}\left(\frac{\rho_l\sigma g}{P_{sat}^2}\right)^{-0.425}(\alpha),\quad G_{gb}=\frac{V}{D_oL}\left(\frac{\rho_l}{\rho_v}\right) \tag{8}$$

In the cases where oil or methanol feed gas were used as cooling media, the relations presented by Kern [21] were used. This correlation was reported for the shell and tube heat exchangers with 60° triangular equilateral pitch tubes that are similar to the geometry of the shell and tube reactors in this study.

$$\frac{h_oD_e}{k_{shell}}=0.36\left(\frac{D_oG_{shell}}{\mu_{shell}}\right)^{0.35}\left(\frac{Cp_{shell}\mu_{shell}}{k_{shell}}\right)^{1/3}\left(\frac{\mu_{shell}}{\mu_w}\right)^{0.14} \tag{9}$$

$$D_e=\frac{4[(0.5P')(0.86P')-0.5\pi LD_o^2/4]}{\frac{\pi D_o}{2}} \tag{10}$$

To calculate heat transfer rate from Eq. (2), besides tube side temperatures, which are found in every section of the reactor by energy balance inside the tube, the shell side temperature and $\Delta H_{rxn}$ are also needed.

With saturated water as the cooling media, the shell side temperature is the saturation temperature of boiling water, but for the other cases, the heat balance equation for the shell side was written as Eq. (11).

$$\frac{dT_{shell}}{dz}=\frac{-N_{tube}q\pi D_i}{\sum_i F_{i,shell}Cp_{i,shell}} \tag{11}$$

where $N_{tube}$ is the number of tubes in the shell and tube reactor. The heat of reaction is calculated through Eq. (12).

$$\Delta H_{rxn}=\Delta H_{298.15\,K}+\int_{298.15}^{T}\Delta Cp\,dT,\quad \Delta Cp=\sum \upsilon_i Cp_i \tag{12}$$

where $\Delta H_{298.15\,K}$ and $\upsilon_i$ are the standard heat of reaction at 298.15 K and the stoichiometric coefficient of the i-th component, respectively.

A number of rate equations for the methanol dehydration reaction have been presented by researchers, but Eq. (13) is more precise for the catalyst used in the industry.

**Table 1. The specifications of reactor, catalyst and feed gas**

| | |
|---|---|
| Reactor material of construction | Stainless steel (thermal conductivity =25 W $m^{-1}$ $k^{-1}$) |
| Catalyst type | $\gamma$-Alumina |
| Catalyst shape | Cylindrical, diameter=length=0.125 inches |
| Catalyst density | 950 Kg/$m^3$ |
| Catalyst bulk density | 632.82 Kg/$m^3$ |
| Feed gas composition | 94.53% Methanol, 3.83% DME, 1.64% $H_2O$ |
| Feed gas mass flow rate | 182,905 Kg/h |
| Feed gas temperature | 260 °C |
| Feed gas pressure | 18.18 bar |

$$r_{DME}=\frac{3.946\times10^{7}\exp\left(\frac{-14070.6}{T}\right)(0.9949P_{MeOH})^{2}(1-\beta)}{\left[1+10^{-8}\exp\left(\frac{2824.3}{T}\right)(0.9949P_{MeOH})+10^{-8}\exp\left(\frac{2503.4}{T}\right)(0.9946P_{H_2O})\right]^{2}}$$

$$\beta=\frac{P_{DME}P_{H_2O}}{P_{MeOH}K_{eq}} \tag{13}$$

$$\ln K_{eq}=0.8695637\ln(T)+\frac{3138.192}{T}-9.077292+1.33\times10^{-3}T-1.23\times10^{-6}T^{2}+3.51\times10^{-10}T^{3}$$

where $P_i$ is the partial pressure of the i-th component.

In Table 1, the specifications of reactor, catalyst and feed gas used in this study are close to the commercial plant specifications.

For an adiabatic reactor, the internal diameter and height of the reactor was 4 m and 8 m, respectively, with a total bed volume of 100 $m^3$. For the non-adiabatic reactor, the shell diameter and bed height of tubular reactor was selected as 5.5 m and 8 m, respectively. A triangular pattern for tubes in the non-adiabatic reactor with a pitch of 2.8 inches was selected, while the internal and external diameters of tubes are 2 inches and 2.2 inches, respectively. The total number of tubes in the reactor shell is 6459. The total reactor bed volume and total heat transfer surface area is 100 $m^3$ and 8119 $m^2$, respectively. The mass flow rate per area of tubes in case of non-adiabatic reactor was considered equal to the mass flow rate per area of the shell in adiabatic reactor (G=4 kg $m^{-2}$ $s^{-1}$).

To solve Eqs. (1)-(3) and Eq. (11) simultaneously, the modified fourth-order Runge-Kutta method was used and the variation of methanol conversion, pressure and shell and tube side temperatures along the tubular reactor were calculated. At first, the values of dx/dz, dP/dz, dT/dz and $dT_{shell}/dz$ were calculated using the feed gas stream conditions (composition, temperature and pressure) and then by applying the Runge-Kutta method, temperature, pressure, conversion, and other variables were calculated in the first increment (dz) of the reactor which were used as the initial values for the second increment.

In case of saturated water as the cooling media, the tubes in the upper section of the shell and tube reactor are in contact with the water vapor, generated in lower section of the reactor. As the rate of heat transfer between water vapor and the tubes in the upper section of the shell and tube reactor is small, the upper section of the reactor was assumed adiabatic. In other words, the reactor was divided into adiabatic and non-adiabatic sections. In addition, the shell side temperature is the saturated temperature of boiling water at shell side pressure which can be controlled by a pressure regulator on the shell side of the reactor.

As the physical properties of reaction media such as thermal conductivity, viscosity and heat capacity vary with temperature, some correlations of these properties as a function of temperature in the temperature range of reactor were made and used in this research. To calculate fluid density, ideal gas and Lee-Kesler equation-of-state (EOS) were used.

## RESULTS AND DISCUSSIONS

### 1. Adiabatic Reactor

The results of reactor modeling, using three different rate equations, and the commercial plant data in terms of methanol conversion along the adiabatic reactor are shown in Fig. 1, which reveals

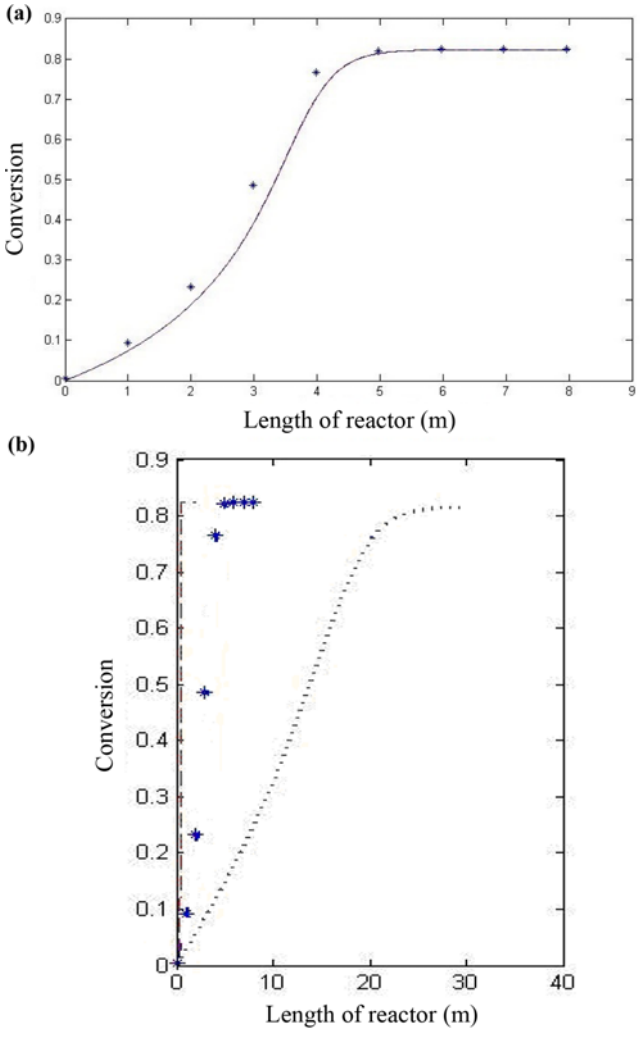


**Fig. 1. Variation of methanol conversion along the adiabatic reactor obtained based on (a) Eq. 13 (—), commercial plant data (*); (b) Mollavali rate equation [17] (- -), Bercic rate equation [15] (. . .), commercial plant data (*).**

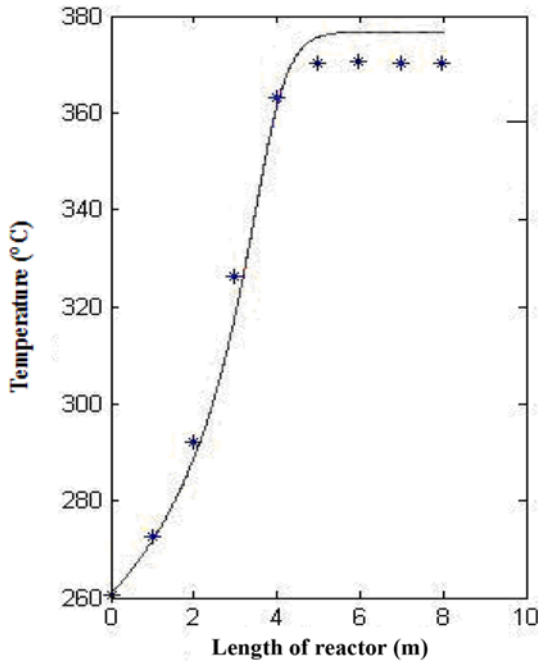


**Fig. 2. Variation of temperature along the adiabatic reactor; Eq. 13 (—), commercial plant data (*).**

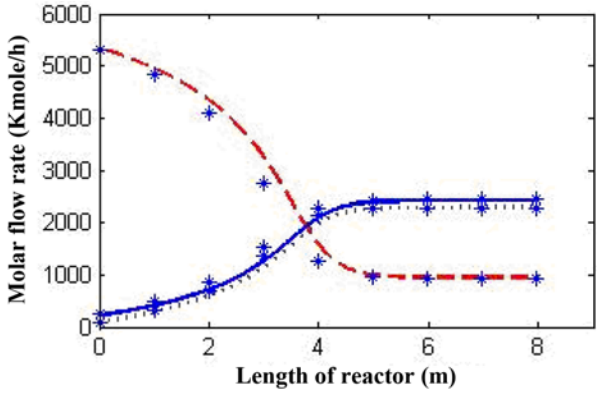


**Fig. 3. Variation of molar flow rate of reaction components along the adiabatic reactor, using Eq. 13. MeOH (- -), DME (—), $H_2O$ (. . .), commercial plant data (*).**

that the methanol conversions predicted by Eq. (13) are closer to the commercial plant data, so this rate equation was used in this research. Furthermore, there are large differences between various rate equations, reported for DME synthesis reaction.

Variation of reaction temperature and the molar flow rate of reaction components along the adiabatic reactor, using Eq. (13), are shown in Figs. 2-3, respectively. Methanol conversion and temperature increase along the reactor and the conversion at the exit of the reactor is 0.82. The results show good agreement with the data obtained from a commercial plant. Due to the assumption of neglecting the side reactions in the reactor modeling, little difference in reaction temperature between the commercial plant data and the results obtained by reactor modeling is observed as shown in Fig. 2.

## 2. Non-adiabatic Reactor

### 2-1. Saturated Water as Cooling Media

Figs. 4-5 depict the variation of temperature and conversion for

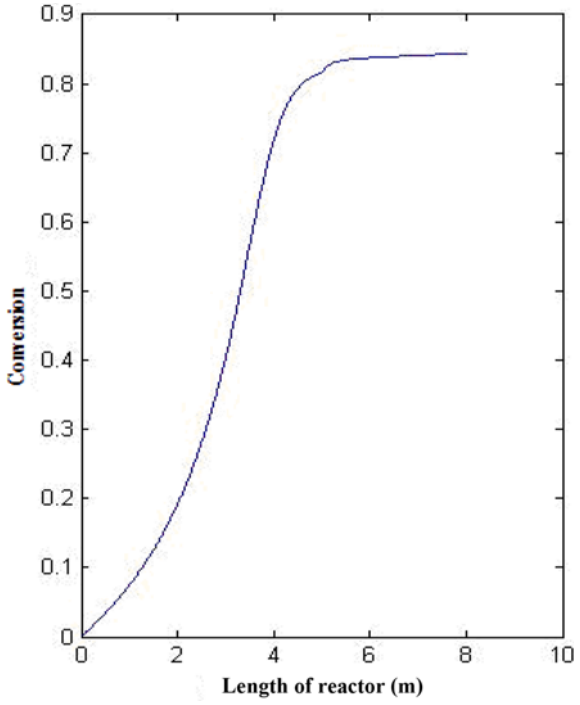


**Fig. 4. Variation of methanol conversion along the non-adiabatic shell and tube reactor; saturated water in the shell side.**

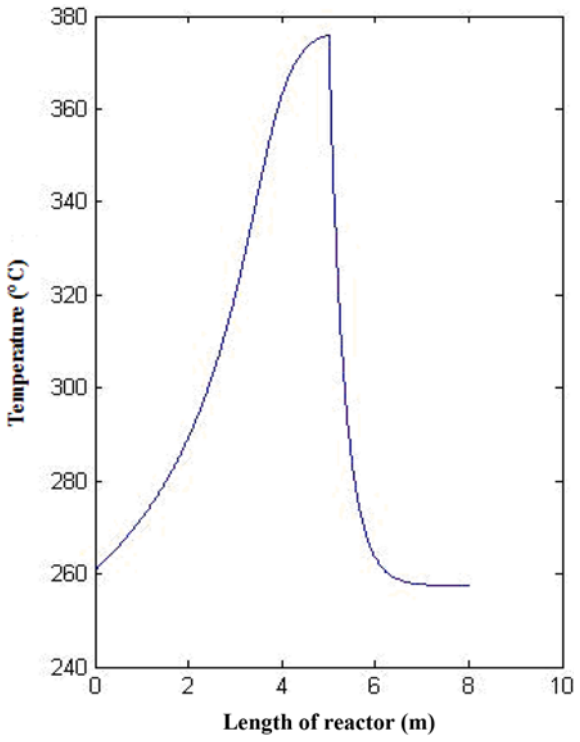


**Fig. 5. Variation of temperature along the non-adiabatic shell and tube reactor; saturated water with a temperature of 255 °C flows in the shell side.**

a non-adiabatic shell and tube reactor where saturated water flows in the shell side of the reactor. Along the adiabatic section of the reactor, where water vapor is in contact with the tubes, an increase in temperature can be observed, while as reaction medium enters

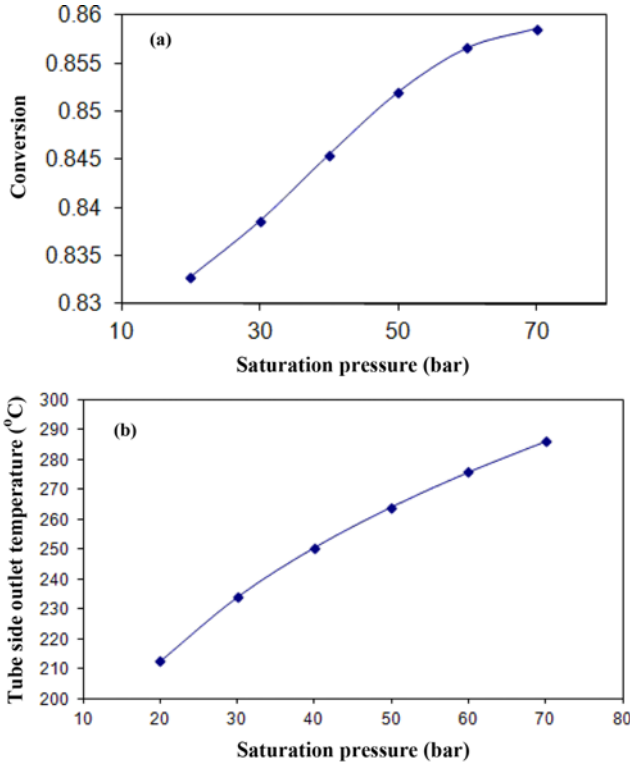


**Fig. 6. Effect of saturated water absolute pressure in the shell side of reactor on: (a) methanol conversion, (b) tube side outlet temperature for a non-adiabatic shell and tube reactor; mass flow rate through tube and shell (G)=4 kg $m^{-2}$ $s^{-1}$, total length of reactor=5 m.**

to the non-adiabatic section, temperature is reduced. The decrease in the temperature leads to the increase in the reaction potential and methanol conversion, as shown in Fig. 4, and at the exit of the reactor the methanol conversion approaches to 0.84, which is higher than the methanol conversion in the adiabatic reactor.

The effect of various parameters, such as temperature of saturated water in the shell side, on methanol conversion and outlet temperature of reactor was investigated. As shown in Figs. 6(a), (b), increasing the temperature and pressure of saturated water in the shell side of the reactor increases the methanol conversion as well as the tube side outlet temperature. When the pressure of saturated water in the shell side of the reactor is less than 40 bar, the tube side outlet temperature approaches to the deactivation temperature of the catalyst. On the other hand, the reactor wall thickness increases by increasing the pressure. So, the shell side absolute pressure of 40 bars (temperature of 255 °C) would be suitable for design of the reactor.

In this study, the length of the adiabatic section of non-adiabatic reactor with saturated water in the shell side is optimized to obtain the maximum conversion of methanol. As shown in Fig. 7, when pressure of saturated water in the shell side is 50 bar and at different total length of the reactor, the optimum adiabatic length of reactor is about 5.3 m. However, when pressures of saturated water in the shell side are 30 and 70 bar, the optimum adiabatic length is about 6 m and 5 m, respectively.

2-2. Methanol Feed Gas Stream as Cooling Media in Co-current Flow Regime

In this case, methanol feed gas is preheated in the shell side of

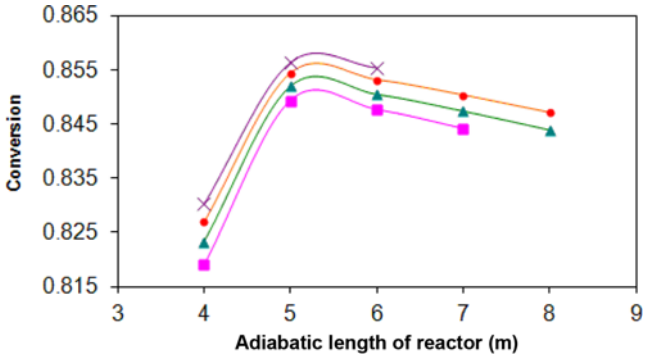


**Fig. 7. Methanol conversion verses the length of adiabatic section of non-adiabatic reactor and at different total length of reactor; pressure of saturated water in the shell side=50 bar; total length of reactor=9 m (■), 10 m (▲), 11 m (●), 12 m (×).**

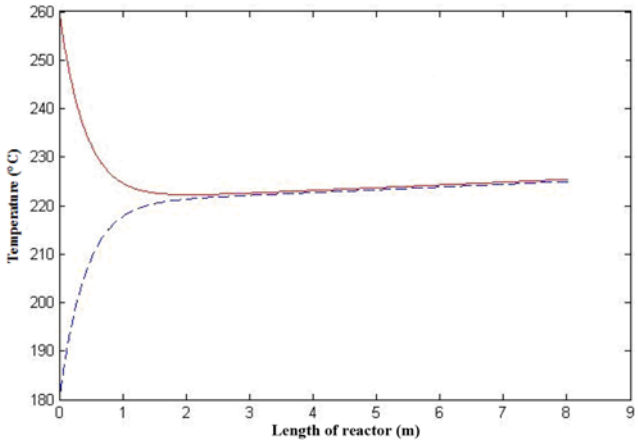


**Fig. 8. Variation of tube side (—) and shell side (- -) temperatures along the reactor.**

the reactor and reaches to inlet temperature of the reactor. In Fig. 8, variation of temperature in this non-adiabatic shell and tube reactor, when methanol feed gas flows co-currently in the shell side of the reactor with an inlet shell side temperature of 180 °C and inlet tube side temperature of 260 °C is shown. Through the heat transferred from tube side to the shell side, the temperature of the tube side is reduced continuously to reach the shell side temperature at the end of the reactor, but through this process, the tube side temperature approaches the deactivation temperature of the catalyst.

The methanol feed gas stream, which is used as a cooling media, will be sent to the tube side of the reactor to be converted to DME. So, to avoid using heat exchangers for cooling or heating of this stream, it is better that the outlet temperature of the shell side be equal to the inlet temperature of the tube side. To achieve this condition, the modeling of reactors with different shell and tube side inlet temperatures was investigated to choose the most suitable inlet temperatures of shell and tube sides.

The effect of shell side inlet temperature on the methanol conversion was investigated for a reactor with a length of 8 m and tube side inlet temperature of 260 °C. The results are presented in Fig. 9, which shows high methanol conversion can be achieved if the shell side inlet temperature is more than 280 °C. Due to the continuous

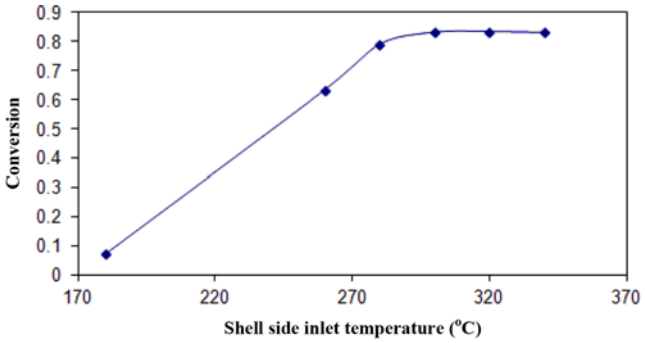


**Fig. 9. Effect of shell side inlet temperature on the methanol conversion; tube side inlet temperature=260 °C, reactor length= 8 m.**

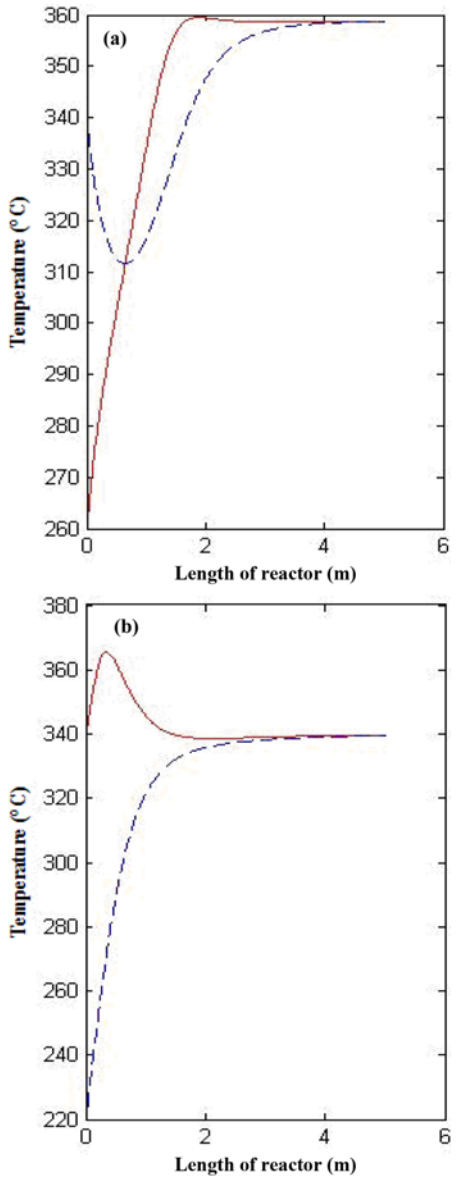


**Fig. 10. Variation of temperature along the non-adiabatic reactor (methanol feed gas stream flows co-currently in the shell side); tube side temperature (—), shell side temperature (- -).**
(a) $T_{in}^{tube}$=260 °C, $T_{in}^{shell}$=340 °C, (b) $T_{in}^{tube}$=340 °C, $T_{in}^{shell}$=220 °C

heat transfer from tube side to shell side and reduction of tube side temperature along the reactor, the rate of reaction decreases, which reduces the methanol conversion.

In Fig. 10, temperature variations in shell and tube sides of the reactor for two cases are shown: $T_{in}^{tube}$=260 °C, $T_{in}^{shell}$=340 °C (Fig. 10(a)) and $T_{in}^{tube}$=340 °C, $T_{in}^{shell}$=220 °C (Fig. 10(b)).

As shown in Fig. 10(a), at the entrance of the reactor, heat is transferred from shell side to the tube side, but as reaction proceeds along the reactor, shell side temperature decreases while tube side temperature increases and the direction of heat transfer is reversed. Since the rate of heat transfer from tube side to shell side is lower than the rate of heat generation by the reaction, temperature increases continuously along the reactor. In this case, the methanol conversion approaches to 0.83 at the exit of reactor (reactor length: 5 m).

As shown in Fig. 10(b), by increasing the inlet temperature of the tube side and decreasing the inlet temperature of the shell side, the outlet temperature of the shell side will be the same as the inlet temperature of the tube side. Moreover, a maximum temperature is observed inside the tube side of the reactor, which should not be more than the sintering temperature of the catalyst. In this case, the methanol conversion approaches to 0.83 at the reactor length of 8 m.

In Fig. 11, the effect of tube side inlet temperature on the tube side outlet temperature, shell side outlet temperature and tube side maximum temperature (which may happen inside the tubes of the reactor), when shell side inlet temperature is 260 °C, is shown. By increasing the tube side inlet temperature, the shell side and tube side outlet temperatures, which are equal at the end of the reactors, increase. Furthermore, the tube side maximum temperature, which occurs inside the tubes when tube side inlet temperature is more than 320 °C, increases. The range of shell side and tube side outlet temperatures is acceptable, but when the tube side inlet temperature is more than 340 °C, the tube side maximum temperature is in the range of sintering temperature of the catalyst.

The effect of mass flow rate through the tubes on methanol conversion, tube and shell side temperatures and tube side maximum temperature is shown in Fig. 12. As mass flow rate through a tube increases, the residence time of reactants in the reactor decreases,

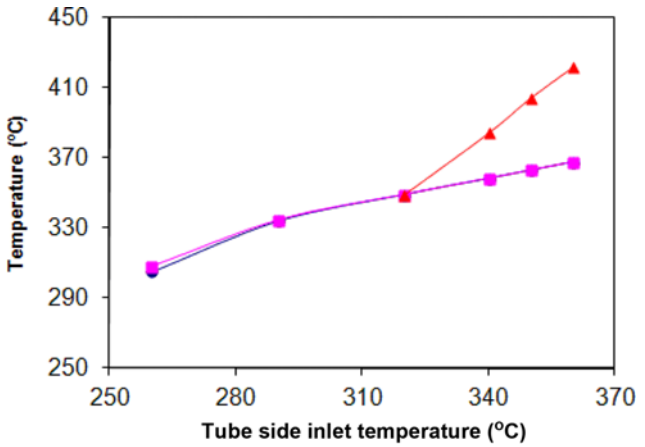


**Fig. 11. The effect of tube side inlet temperature on tube side outlet temperatures (■), shell side outlet temperature (●) and tube side maximum temperature (▲); shell side inlet temperature=260 °C.**

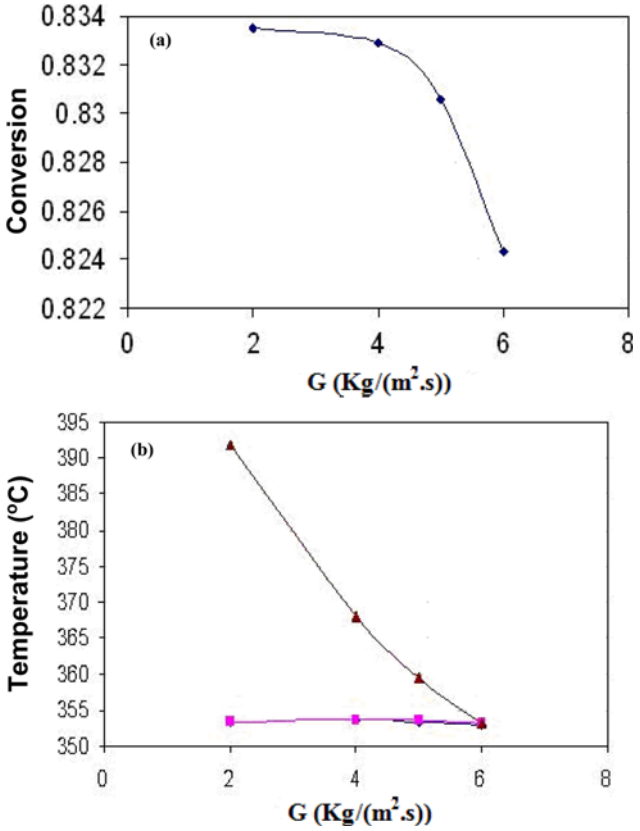


**Fig. 12. The effect of mass flow rate per unit area of tubes on (a) methanol conversion (b) tube side (■) and shell side (●) outlet temperatures and tube side maximum temperature (▲).**

which reduces the methanol conversion. On the other hand, as the total mass flow rate of reactants is constant, reducing the mass flow rate through a tube increases the number of tubes in the reactor. Furthermore, as presented in Fig. 12(b), reduction of mass flow rate through a tube increases the tube side maximum temperature; e.g., for G=2 kg $m^{-2}$ $s^{-1}$, the tube side maximum temperature approaches the sintering temperature of the catalyst. Therefore, considering the slight increase in methanol conversion for mass flow rate less than 4 kg $m^{-2}$ $s^{-1}$, G=4 kg $m^{-2}$ $s^{-1}$ was considered as the optimum mass flow through the tube.

2-3. Methanol Feed Gas Stream as Cooling Media in Counter Current Flow Regime

In Figs. (13-14), variation of methanol conversion and tube and shell sides temperatures in the non-adiabatic reactor, which methanol feed gas stream flows counter currently in the shell side of the reactor, are shown. Similar to the previous case (section 2.2) and to avoid using heat exchangers in the DME production process to heat or cool the streams, the optimum shell side inlet temperature is about 180 °C. However, based on the modeling results, the tube side outlet temperature will be less than 260 °C. Therefore, as shown in Fig. 14, the shell side inlet temperature was increased to 200 °C to increase the tube side outlet temperature. The methanol conversion at the exit of the reactor, when the total length of the reactor is 3 m, is about 0.82 and increases by increasing the total length of reactor but in this case, the tube side outlet temperature will be less than 260 °C.

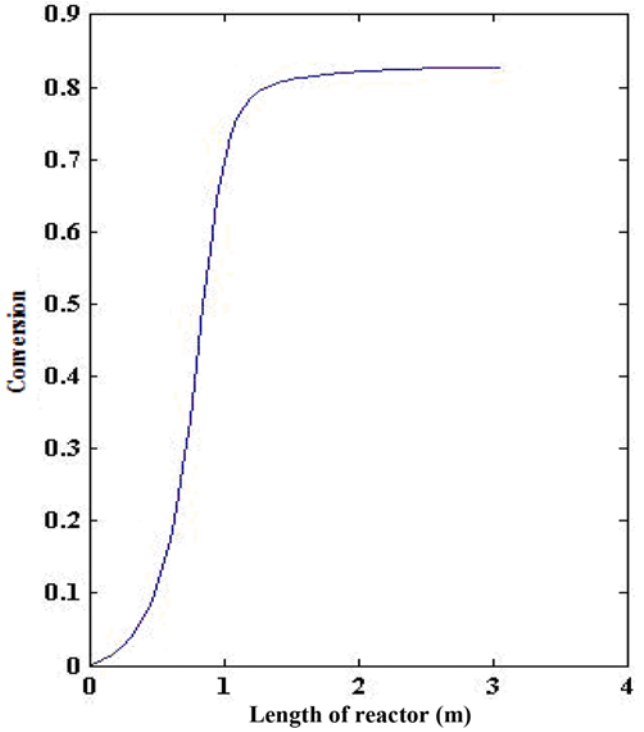


**Fig. 13. Variation of methanol conversion along the non-adiabatic reactor; methanol feed gas stream flows counter currently in the shell side.**

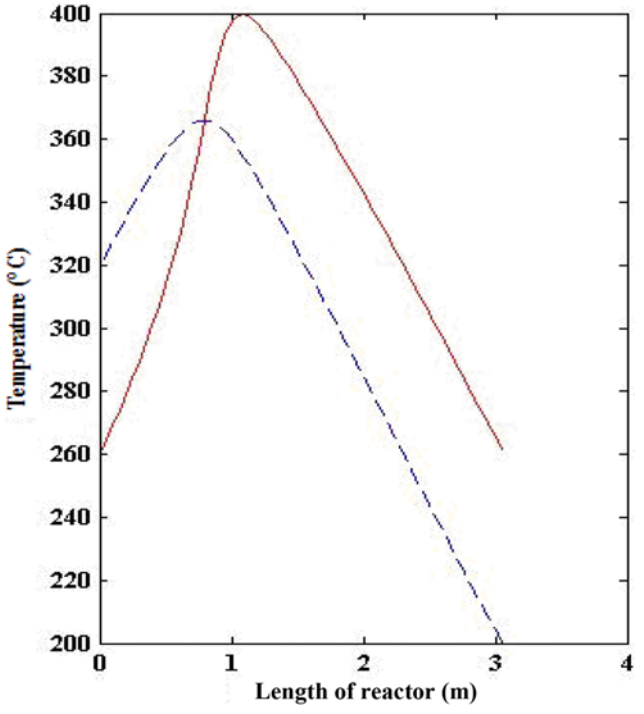


**Fig. 14. Variation of temperature along the non-adiabatic reactor, methanol feed gas stream flows counter currently in the shell side; tube side temperature (—), shell side temperature (- -).**

In this case, the feed gas stream is preheated in the shell side of the reactor and reaches the inlet temperature of the reactor. Even

though a bigger reactor is needed, the costs for heating medium and heat exchanger to heat the feed gas stream will be eliminated. Moreover, due to the deactivation of catalyst, the tube side temperature needs to be controlled in the range of 260 to 380 °C. Thus, the low heat capacity of the gas stream in comparison with the liquid water stream is an advantage, because the gas cooling medium prevents the reduction of tube side temperature less than 260 °C and controls the tube side temperature in the before mentioned temperature range.

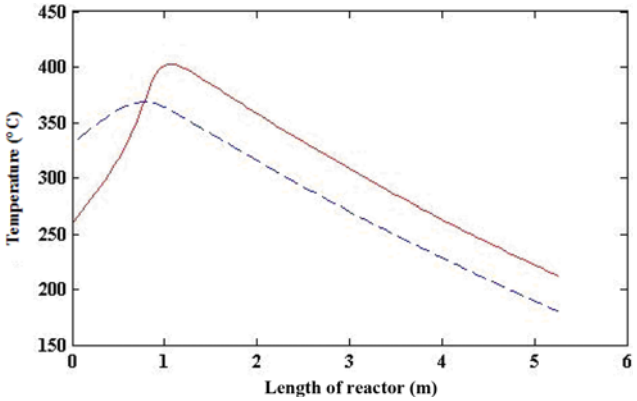


**Fig. 15. Variation of temperature along the non-adiabatic reactor, cooling oil flows counter currently in shell side; tube side temperature (—), shell side temperature (- -).**

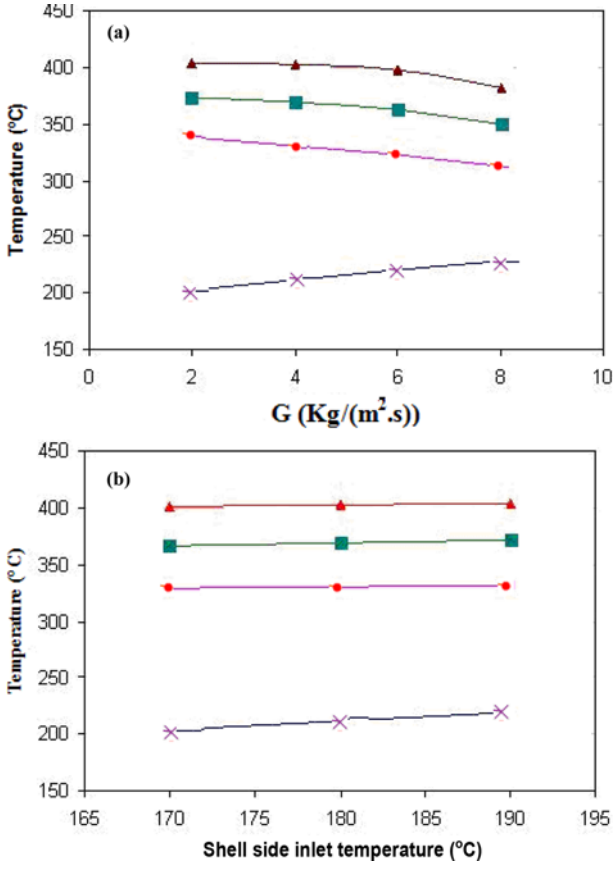


**Fig. 16. Effects of various parameters on $T_{tube}^{out}$ (×), $T_{shell}^{out}$ (●), $T_{tube}^{max}$ (▲) and $T_{shell}^{max}$ (■), (a) mass flow rate per unit area of tube (b) shell side inlet temperature.**

2-4. Oil as Cooling Media in Counter Current Flow Regime

In Fig. 15, temperature variation in non-adiabatic reactor, where cooling oil flows counter currently in the shell side of the shell and tube reactor, is shown. A maximum in the both tube side and shell side temperatures is observed, which the maximum temperature for tube side is higher than 400 °C and also, the tube side outlet temperature is lower than 250 °C. Both temperatures are in the range of catalyst deactivation, and in contrast to the previous cases (methanol feed gas stream in the shell side, section 2.2 and section 2.3), the reactor temperature cannot be adjusted to the suitable range by changing the different parameters.

The effect of mass flow rate per unit area of tube on the tube and shell side temperatures was investigated. According to Fig. 16(a), although the tube side maximum temperature at G=8 kg $m^{-2}$ $s^{-1}$ is less than sintering temperature of the catalyst, the tube side outlet temperature is in the temperature range of catalyst deactivation. Moreover, Fig. 16(b) demonstrates that increasing the shell side inlet temperature does not lead to the tube side outlet temperature being more than the deactivation temperature of catalyst. Therefore, although more methanol conversion can be achieved in lower length of a reactor with oil as cooling media, because of the temperature limits, this case is not acceptable.

In this research, the effect of different equation of state on the results was investigated. The results show that there are no significant differences between the modeling results based on the two different equation-of-state, ideal gas and Lee-Kesler. Therefore the reaction mixture was assumed to be an ideal gas mixture.

## CONCLUSION

In an adiabatic DME synthesis reactor, increasing the reactor temperature leads to the decrease in the equilibrium conversion. Based on the results of the present research, by using a non-adiabatic reactor and control of the reactor temperature, more methanol conversion at the exit of the reactor can be achieved. Considering the temperature limitations, regarding the catalyst deactivation and among the investigated cases, non-adiabatic reactors with saturated water or feed gas stream in the shell side present better results than the adiabatic reactor; e.g., in case of saturated water in the shell side of the reactor as cooling media, the methanol conversion increases by 4%, compared to adiabatic reactor. However in some cases, heat exchangers should be added to the DME production process. In the case which cooling oil flows countercurrently in the shell side of the reactor, tube side temperature increases more than the sintering temperature of the catalyst, and then decreases lower than the deactivation temperature of the catalyst. Therefore, this case is not acceptable. Moreover, the results of adiabatic reactor modeling show good agreement with the data from a commercial plant.

## NOMENCLATURE

$A_i$ : internal cross sectional area of tubes
$A_o$ : external cross sectional area of tubes
$CP_i$ : specific heat capacity of i-th component in the tube side stream
$Cp_l$ : specific heat capacity of liquid water
$D_i$ : internal diameter of tubes
$D_o$ : external diameter of tubes

$D_p$ : equivalent diameter of catalyst particles
$F_i$ : molar flow rate of the i-th component in the tube side stream
$F_{mo}$ : feed methanol molar flow rate
G : mass velocity of tube side stream per unit area of tubes
$G_{gb}$ : mass velocity of liquid water per projected area of tube
g : acceleration of gravity
$h_i$ : heat transfer coefficient in the tube side
$h_o$ : heat transfer coefficient in the shell side
$h_b$ : bed heat transfer coefficient
$h_w$ : wall heat transfer coefficient
$\Delta H_{rxn}$ : heat of reaction
$\Delta H_{298.15\,K}$ : standard heat of reaction at 298.15 °K
K : thermal conductivity of tube
k : thermal conductivity of tube side stream
$k_l$ : thermal conductivity of liquid water
$K_{eq}$ : equilibrium constant of reaction
$k_{er}$ : radial effective thermal conductivity
L : length of reactor
$N_{tube}$ : number of tubes
$Nu_w$ : Nusselt number ($h_w D_p/k$)
P : total pressure
P′ : tube pitch
$P_{sat}$ : saturation pressure of boiling water
$P_i$ : partial pressure of component i
Pr : Prandtl number ($C_p\mu/k$)
q : transferred heat per unit area
r : rate of reaction
R : radius of bed
$Re_p$ : Reynolds number, ($GD_p/\mu$)
T : temperature
U : overall heat transfer coefficient
V : mass velocity of vapor produced
x : methanol conversion
z : length

**Greek Letters**

$\alpha$ : surface condition factor (1.7 for average tube condition)
$\rho_B$ : bulk density of catalyst bed
$\rho_f$ : density of tube side stream
$\rho_l$ : density of liquid water (at saturation temperature)
$\rho_v$ : density of water vapor (at saturation temperature)
$\sigma$ : surface tension of liquid
$\xi$ : void fraction of catalyst bed
$\mu$ : viscosity of tube side stream
$\mu_w$ : shell side viscosity near wall
$\mu_l$ : viscosity of liquid water
$\phi$ : metal type factor, 0.00059 for stainless steel
$\upsilon_i$ : stoichiometric coefficient of i-th component

**Subscripts**

DME : di-methyl-ether component
MeOH : methanol component
shell : shell side
tube : tube side

## REFERENCES


1. C. Arcoumanis, C. Bae, R. Crookes and E. Kinoshita, *Fuel*, **87**, 1014 (2008).
2. A. M. Arkharov, S. D. Glukhov, L. V. Grekhov, A. A. Zherdev, N. A. Ivashchenko, D. N. Kalinin, A. V. Sharaburin and A. A. Aleksandrov, *Chem. Petro. Eng.*, **39**, 330 (2003).
3. K. L. Ng, D. Chadwick and B. A. Toseland, *Chem. Eng. Sci.*, **54**, 3587 (1999).
4. S. B. Lee, W. Cho, D. K. Park and E. S. Yoon, *Korean J. Chem. Eng.*, **23**, 522 (2006).
5. G. X. Qi, X. M. Zheng, J. H. Fei and Z. Y. Hou, *J. Mol. Catal. A: Chem.*, **176**, 195 (2001).
6. K. Sun, W. Lu, F. Qiu, S. Liu and X. Xu, *Appl. Catal., A*, **252**, 243 (2003).
7. W. Z. Lu, L. H. Teng and W. D. Xiao, *Chem. Eng. Sci.*, **59**, 5455 (2004).
8. F. Raoof, M. Taghizadeh, A. Eliassi and F. Yaripour, *Fuel*, **87**, 2967 (2008).
9. M. Xu, J. H. Lunsford, D. W. Goodman and A. Bhattacharyya, *Appl. Catal., A*, **149**, 289 (1997).
10. G. Moradi, F. Yaripour, H. Abbasian and M. Rahmanzadeh, *Korean J. Chem. Eng.*, **27**(5), 1435 (2010).
11. D. Liu, X. Hua and D. Fang, *J. Nat. Gas Chem.*, **16**(2), 193 (2007).
12. Y. Hu, Z. Niel and D. Fang, *J. Nat. Gas Chem.*, **17**, 195 (2008).
13. Y. Ono and T. Mori, *J. Chem. Soc. Faraday Trans. 1*, **77**, 2209 (1981).
14. T. R. Forester and R. F. Howe, *J. Am. Chem. Soc.*, **109**, 5076 (1987).
15. G. Bercic and J. Levec, *Ind. Eng. Chem. Res.*, **32**, 2478 (1993).
16. W. Z. Lu, L. H. Teng and W. D. Xiao, *Chem. Eng. Sci.*, **59**, 5455 (2004).
17. M. Mollavali, F. Yaripour, H. Atashi and S. Sahebdelfar, *J. Am. Chem. Soc.*, **47**, 3265 (2008).
18. K. S. Ha, Y. J. Lee, J. W. Bae, Y. W. Kim, M. H. Woo, H. S. Kim, M. J. Park and K. W. Jun, *Appl. Catal. A: Gen.*, **395**, 95 (2011).
19. C. H. Li and B. A. Finlayson, *Chem. Eng. Sci.*, **32**, 1055 (1997).
20. C. H. Gilmour, *Chem. Eng. Prog.*, **54**(10), 77 (1958).
21. D. Q. Kern, *Process heat transfer*, 1st Ed., McGraw-Hill Inc., New York, NY (1950).